nature food

ARTICLES

https://doi.org/10.1038/s43016-021-00341-6

Check for updates

Stronger temperature–moisture couplings exacerbate the impact of climate warming on global crop yields

Corey Lesk [1,2] ✉, Ethan Coffel [3], Jonathan Winter [4], Deepak Ray [5], Jakob Zscheischler [6,7,8], Sonia I. Seneviratne [9] and Radley Horton [1]

Rising air temperatures are a leading risk to global crop production. Recent research has emphasized the critical role of moisture availability in regulating crop responses to heat and the importance of temperature–moisture couplings in driving concurrent heat and drought. Here, we demonstrate that the heat sensitivity of key global crops depends on the local strength of couplings between temperature and moisture in the climate system. Over 1970–2013, maize and soy yields dropped more during hotter growing seasons in places where decreased precipitation and evapotranspiration more strongly accompanied higher temperatures, suggestive of compound heat–drought impacts on crops. On the basis of this historical pattern and a suite of climate model projections, we show that changes in temperature–moisture couplings in response to warming could enhance the heat sensitivity of these crops as temperatures rise, worsening the impact of warming by −5% (−17 to 11% across climate models) on global average. However, these changes will benefit crops where couplings weaken, including much of Asia, and projected impacts are highly uncertain in some regions. Our results demonstrate that climate change will impact crops not only through warming but also through changing drivers of compound heat–moisture stresses, which may alter the sensitivity of crop yields to heat as warming proceeds. Robust adaptation of cropping systems will need to consider this underappreciated risk to food production from climate change.

Several studies have identified negative relationships between air temperature and crop yields in observations, signalling the potential for global warming to reduce agricultural output[1–3]. Extreme heat can steeply reduce crop yields both directly through heat stress and indirectly by raising atmospheric vapour demand and contributing to moisture stress[2,4–8]. Because of this dual effect, the impacts of extreme heat are typically amplified by drought and can be minimized with sufficient soil moisture from either precipitation or irrigation[7,9–16]. Jointly hot and dry conditions thus pose a particular climate risk to global crops, especially under global warming[17].

In many regions, such jointly hot and dry conditions during cropping seasons tend to occur due to physical couplings between temperature and moisture in the climate system[18–20]. These couplings can be conceptualized in two ways: first as a connection between temperature (T) and precipitation (p), and second as a connection between T and evapotranspiration (ET). We refer to the former connection as the atmospheric circulation coupling and the latter as the land–atmosphere interaction coupling. While the separability and relative importance of these two couplings is debated[18,21,22] (Methods), they generally reflect two critical sets of processes that vary in magnitude over global croplands and strongly influence the local risk of joint heat and drought.

Where the atmospheric circulation coupling is strong, clear skies tend to accompany dry cropping seasons, boosting temperatures at the surface due to increased penetration of solar radiation and delivery of warm compressed air by descending winds[18,20,21,23]. The strength of this coupling is reflected by the magnitude of the negative correlation between temperature and precipitation across years ($r_{T,p} < 0$). Where the land–atmosphere coupling is strong, ET tends to decline during a warmer cropping season, reflected by a negative correlation between T and ET ($r_{T,\mathrm{ET}} < 0$). The resulting enhanced sensible heating can further raise air temperatures and atmospheric vapour demand, generating a positive feedback[19,22,24,25]. By contrast, enhanced ET from warmth ($r_{T,\mathrm{ET}} > 0$) limits the feedback between warming and drying. The couplings characterized by negative correlations of T with ET and p thus drive concurrent and mutually reinforcing hot and dry conditions during the cropping season in many regions.

Despite the importance of these couplings in controlling the concurrent heat and moisture stresses that so strongly damage crop yields, their effect on global crop responses to current and future temperatures remains a gap in understanding present and future climate impacts on crops. Here, we demonstrate the global influence of temperature–moisture couplings on crop yield sensitivity to temperature over 1970–2013 and project future impacts on crops from changing couplings. We combine historical global yield observations[26,27] with observed and modelled meteorological data to show that during warmer growing seasons, maize and soybean yields drop more steeply where precipitation and ET tend to also decrease. Using simulations from a suite of climate models, we then identify how these couplings are likely to change by the late twenty-first

[1]Lamont-Doherty Earth Observatory, Palisades, NY, USA. [2]Department of Earth and Environmental Science, Columbia University, New York, NY, USA. [3]Department of Geography and the Environment, Syracuse University, Syracuse, NY, USA. [4]Department of Geography, Dartmouth College, Hanover, NH, USA. [5]Institute on the Environment, University of Minnesota, St. Paul, MN, USA. [6]Climate and Environmental Physics, University of Bern, Bern, Switzerland. [7]Oeschger Centre for Climate Change Research, University of Bern, Bern, Switzerland. [8]Department of Computational Hydrosystems, Centre for Environmental Research—UFZ, Leipzig, Germany. [9]Institute for Atmospheric and Climate Science, ETH Zürich, Zürich, Switzerland. ✉e-mail: lesk@ldeo.columbia.edu

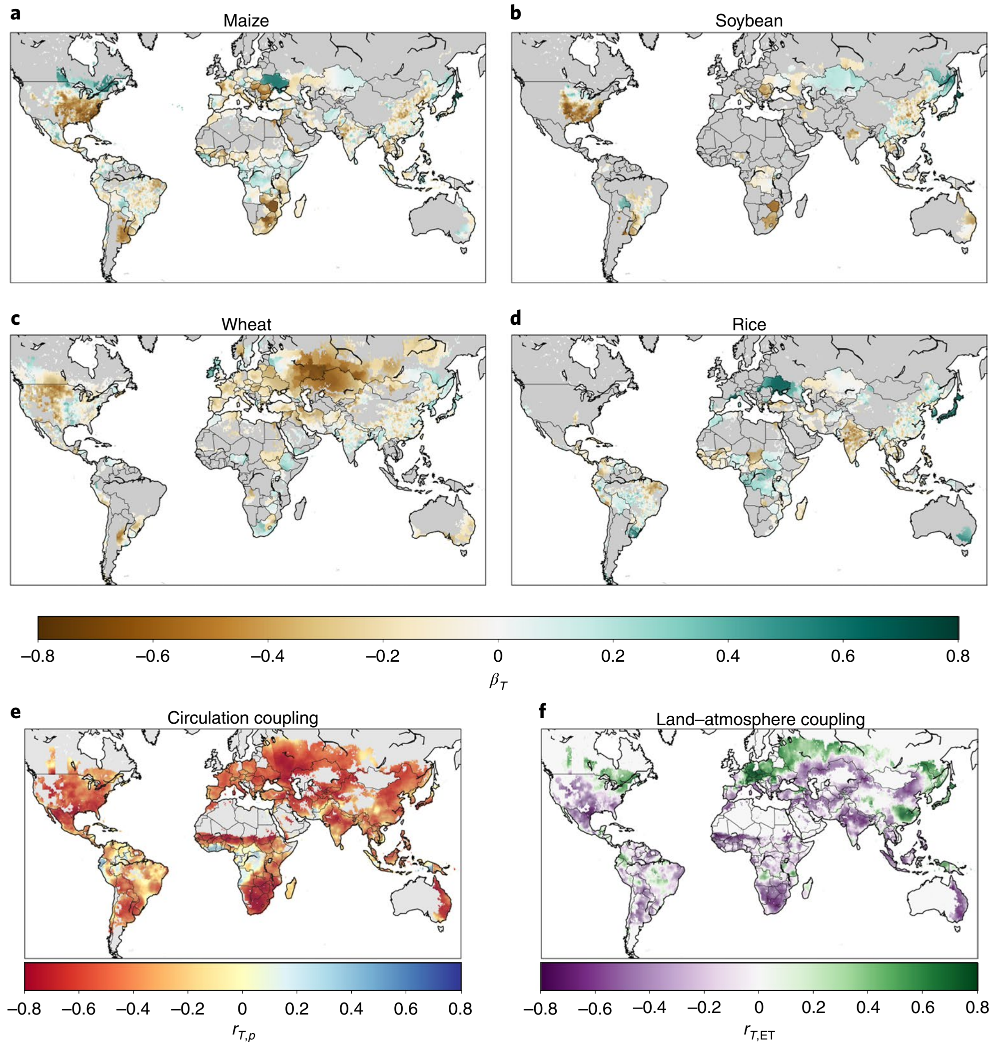

Fig. 1 | Crop yield sensitivity to temperature and temperature–moisture couplings across global croplands. a–d, Standardized yield sensitivity to mean growing season maximum air temperature estimated as the linear slope coefficient (β_T), with units of σ of yield per σ of temperature, for maize (**a**), soybean (**b**), wheat (**c**) and rice (**d**). The yield and temperature observational data are detrended to remove long-term warming and yield trends. Stippling denotes significant slope coefficients (two-tailed $P<0.1$, t-test). Land area without crops is shown in grey. **e**, Circulation coupling strength, measured as the interannual correlation between detrended observed growing season mean temperature and total precipitation ($r_{T,p}$). **f**, Land–atmosphere coupling, measured as the interannual correlation between detrended modelled growing season mean temperature and ET ($r_{T,ET}$). The couplings in **e** and **f** are shown for the maize growing season and over the full global cropland where data are available to ease the interpretation of global patterns. Couplings for other growing seasons are shown in Supplementary Fig. 1.

century. Combining these projections with the historical results, we demonstrate that the modified couplings will probably worsen the impacts of warming on some of the world's most important crops.

Results and discussion

Historical influence of temperature–moisture couplings on crop heat sensitivity. Over the historical period, we find significant correlations between crop yields and mean seasonal temperature over 20–32% of global maize, soybean, rice and wheat croplands ($P<0.1$, Fig. 1). While maize and soybean yields generally decline with increasing temperature (by 0.3–0.4 standard deviations (σ) per σ of temperature), they benefit from heat over around a quarter of croplands with significant temperature impacts, primarily at higher latitudes and elevations as well as in pockets of the tropics (Fig. 1a,b). Yield benefits from warmer seasons in some locations probably reflect crop limitations by cold and short growing seasons. By contrast, wheat yields are almost universally reduced by higher temperatures in North America and Eurasia (Fig. 1c), probably reflecting the lower physiological heat tolerance of wheat compared with maize[28,29]. While seasonal heat benefits rice yields in parts of Europe and damages them slightly in India, rice yields show a generally weaker connection to temperature (Fig. 1d), as reported elsewhere[1,30]. This may relate to the prevalence of irrigation in rice cropping, which may partially decouple yields from temperature. We also note weak maize yield dependence on temperature where it is mainly irrigated such as in northern India, central France and the western United States (Fig. 1a).

Large portions of the global croplands also experience significant temperature–moisture coupling during the local growing season. Seasonal total precipitation is significantly correlated with mean temperature over 62–89% of cropland ($P<0.1$, Fig. 1e and Supplementary Fig. 1), with exceptions mainly concentrated in the tropics. These significant interannual correlations are almost entirely negative (>98%), with a mean magnitude of −0.5. ET

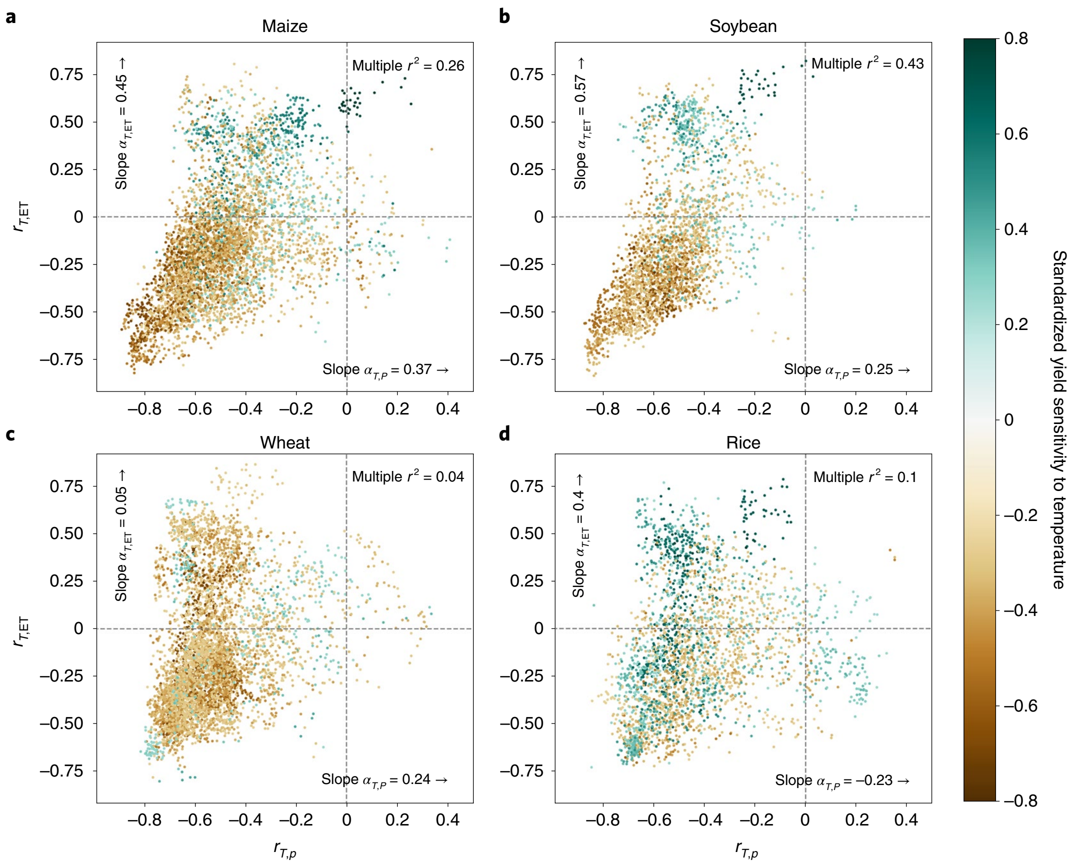

Fig. 2 | Global dependence of yield sensitivity to temperature on two temperature–moisture couplings. a–d, Estimated standardized yield sensitivity to mean growing season maximum air temperature (colouring of the points) plotted in relation to correlations of temperature with ET (land–atmosphere coupling, *y* axes) and precipitation (circulation coupling, *x* axes), for maize ($n = 4{,}771$ grid cells) (**a**), soybean ($n = 2{,}663$) (**b**), wheat ($n = 5{,}062$) (**c**) and rice ($n = 2{,}800$) (**d**). Each data point represents one grid cell. Data are shown for areas with significant yield response to temperature (two-tailed $P < 0.1$). The slope coefficients relating yield sensitivity to each coupling ($\alpha_{T,p}$ and $\alpha_{T,\mathrm{ET}}$) are annotated on their respective axes, with arrows showing the direction in the plot plane to which the slopes apply. The reported multiple r^2 values are for the multiple regression model relating yield sensitivity to the two couplings.

further correlates with temperature over 36-65% of global croplands ($P < 0.1$, Fig. 1f and Supplementary Fig. 1). These correlations are predominantly negative over global croplands but are positive at higher latitudes as well as in southern China (Fig. 1f), a pattern corresponding broadly to moisture-limited versus energy-limited soil moisture regimes[19], respectively. The majority of global cropland area thus experiences climate couplings whereby lower-moisture conditions coincide with higher heat and moisture demand.

We find a global tendency for increasingly negative impacts of temperature on maize and soybean yields with the increasing strength of these temperature–moisture couplings historically. Figure 2 situates the grid-cell yield sensitivity to temperature (presented as the colouring of the points) with respect to the local strength of the two temperature–moisture couplings (presented as the position in the plane of the points). The lower-left quadrant of each panel includes grid cells with both circulation and land–atmosphere couplings ($r_{T,p}$ and $r_{T,\mathrm{ET}} < 0$). For maize and soy (Fig. 2a,b), we note that this quadrant contains the bulk of grid cells where yields decline with temperature, with the greatest negative yield sensitivities where the couplings are strongest. Meanwhile, yields tend to benefit from warmer temperatures where the couplings are weakest ($r_{T,p} \approx 0$ and $r_{T,\mathrm{ET}} > 0$).

To quantify these relationships, we regress crop yield sensitivity to temperature on the two couplings and find meaningful global dependence for maize and soy ($r^2 = 0.26$ for maize and 0.43 for soybean, Fig. 2a,b). The regression also affords slope coefficient estimates, $\alpha_{T,p}$ and $\alpha_{T,\mathrm{ET}}$, that quantify the steepness of the dependence of yield sensitivity to temperature on each of the two couplings. On average, yields decline more steeply per σ of temperature ($\alpha_{T,\mathrm{ET}} \pm$ standard error is 0.45 ± 0.02 for maize and 0.57 ± 0.02 for soybean, $P < 0.001$) in areas with the most negative $r_{T,\mathrm{ET}}$. In other words, crops are around 40% more sensitive to temperature (34% for maize and 43% for soybean) in regions with strong land–atmosphere coupling, compared with regions where temperature and ET are uncorrelated. The influence of the land–atmosphere coupling on yield sensitivity to temperature is somewhat larger than the influence of circulation coupling on yield sensitivity to temperature ($\alpha_{T,p} \pm$ standard error is 0.37 ± 0.03 for maize and 0.25 ± 0.04 for soybean, $P < 0.001$). We found no spatial correlation between recent ten-year mean yields (2004–2013) and the two couplings ($r^2 < 0.02$), suggesting that the observed effects are independent of mean crop productivity. Overall, these patterns of higher crop heat sensitivity where couplings are strong is consistent with the compounding of heat impacts on crops by moisture effects where these couplings are strong, and alleviation where they are weak.

By contrast, we find little such dependence on temperature–moisture couplings among the temperature sensitivities of wheat and rice (Fig. 2c,d, $r^2 \leq 0.1$). This may be due in part to the low thermal tolerance of wheat, whose optimal growth temperature is about 10 °C cooler than that of the other crops[28,29]. Due to its exponential dependence on temperature, atmospheric vapour demand and its impact on crops increase most strongly at relatively high

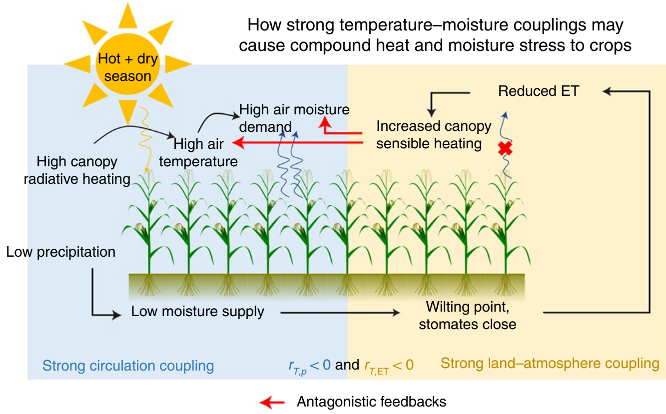

Fig. 3 | Schematic of potential mechanisms for compound heat and moisture impacts on crops in regions with strong temperature–moisture couplings. Where temperature–moisture couplings are strong, hot growing seasons are more likely to also be dry, depicted by the sun at upper left. The ensuing effects of consequence to crops that are linked to strong circulation coupling ($r_{T,p} < 0$) are shown in the blue square (left), while effects linked to strong land-atmosphere coupling ($r_{T,ET} < 0$) are shown in the yellow square (right). The red arrows show antagonistic feedbacks by which correlations of T with p and ET can induce compounding heat and moisture stresses on crops.

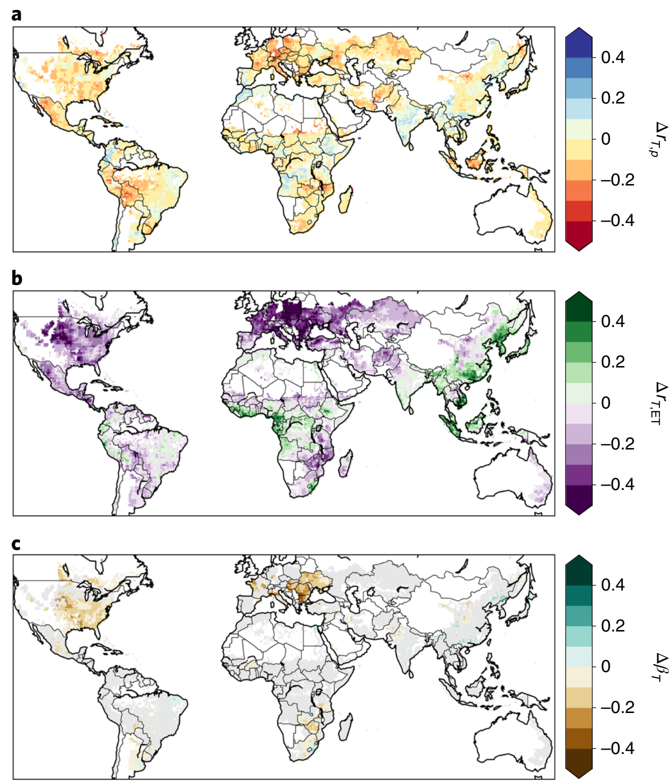

Fig. 4 | Projected future changes in temperature–moisture couplings and yield sensitivity to temperature in response to warming. a, Projected change in circulation coupling (detrended interannual $r_{T,p}$) over 2051–2100 under a moderate-emissions scenario (SSP2-4.5), compared with historical couplings over 1961–2010. The median of an ensemble of 12 CMIP6 climate model projections is shown for each grid cell. **b**, Same as **a**, but for land–atmosphere coupling ($r_{T,ET}$). **c**, Projected change in standardized maize yield sensitivity to temperature in response to changes in the two couplings, based on the global slope coefficients in Fig. 2a. In **a** and **b**, the projections are shown over the full global maize croplands to facilitate the interpretation of broader patterns; in **c**, the projections are shown only for areas with significant historical maize yield sensitivity to temperature ($P < 0.1$). The grey shading shows croplands with insignificant yield dependence on temperature.

temperatures. However, heat impacts on wheat may be severe at relatively low temperatures, at which atmospheric vapour demand remains relatively low, limiting the scope for the compounding of heat impacts by moisture[31]. For rice, lower heat sensitivity and widespread irrigation may effectively decouple the crop from temperature and moisture (Fig. 1d), similarly precluding compounding impacts[30].

These results suggest that local crop responses to temperature depend not only on crop physiology and temperature stressors but also on climatological couplings between temperature and moisture. These couplings tend to align heat and moisture stress in time, exposing crops to heat and high atmospheric moisture demand while precipitation and soil moisture are low (Fig. 3). Where the couplings are strong, yields are probably more sensitive to temperature due to antagonistic feedbacks between physiological heat and drought acclimation and stress mechanisms[8,32], notably the impact of stomatal closure on canopy temperature and photosynthesis[8,16,33–37] (Fig. 3). By contrast, where the couplings are weak, heat and high atmospheric moisture demand are more likely to coincide with periods of normal or abundant precipitation and soil moisture, mitigating the impact of heat on crops.

Importantly, these results indicate that the ultimate impact of global warming on some crops will depend not only on the mounting heat hazard itself but also on the impact of warming on the physical coupling between temperature and moisture. Specifically, they raise the possibility that climate change will affect the sensitivity of crop yields to heat by altering temperature–moisture couplings throughout the world. This potential impact is currently omitted from climate risk projections using statistical models[3,4,6], which assume constant temperature sensitivity into the future, and mechanistic crop models, whose climate projection inputs are typically adjusted to match the historical correlation structure between temperature and moisture[3,38], excluding the potential influence of changes in temperature–moisture couplings.

Impacts of projected changes in couplings on global crop yields. To examine the implications of these effects for maize and soy under future climate change, we combine the historical dependence of yield sensitivity to temperature on the two couplings (Fig. 2) with simulated future changes in couplings from a suite of 12 Coupled Model Intercomparison Project 6 (CMIP6) global climate models[39]. By 2051–2100 under moderate greenhouse gas emissions (Shared Socio-economic Pathway (SSP) 2-4.5), we project substantial changes in $r_{T,ET}$ and smaller changes in $r_{T,p}$ (Fig. 4a,b) over much of global croplands in the ensemble median. These changes indicate amplified couplings between temperature and moisture in response to climate warming over croplands in the United States, Europe and southeastern Africa, but reduced couplings across southern to eastern Asia. On the basis of the historical relationships in Fig. 2a,b, these changes in couplings will probably exacerbate yield sensitivity to temperature over a preponderance of croplands but alleviate it in much of Asia (Fig. 4c).

We project that such heightened crop heat sensitivities due to changing temperature–moisture couplings will worsen the impacts of warming on maize and soy yields across most of the globe (Fig. 5a and Supplementary Fig. 2). In the multimodel median, these additional yield impacts ($\Delta\Delta Y$) amount to regional maize (soy) losses of 7% (9%) in the United States, 7% (16%) in western Europe, 12% (24%) in eastern Europe, 9% (5%) in southeastern Africa and 3% (6%) in southeastern South America, with more modest yield gains

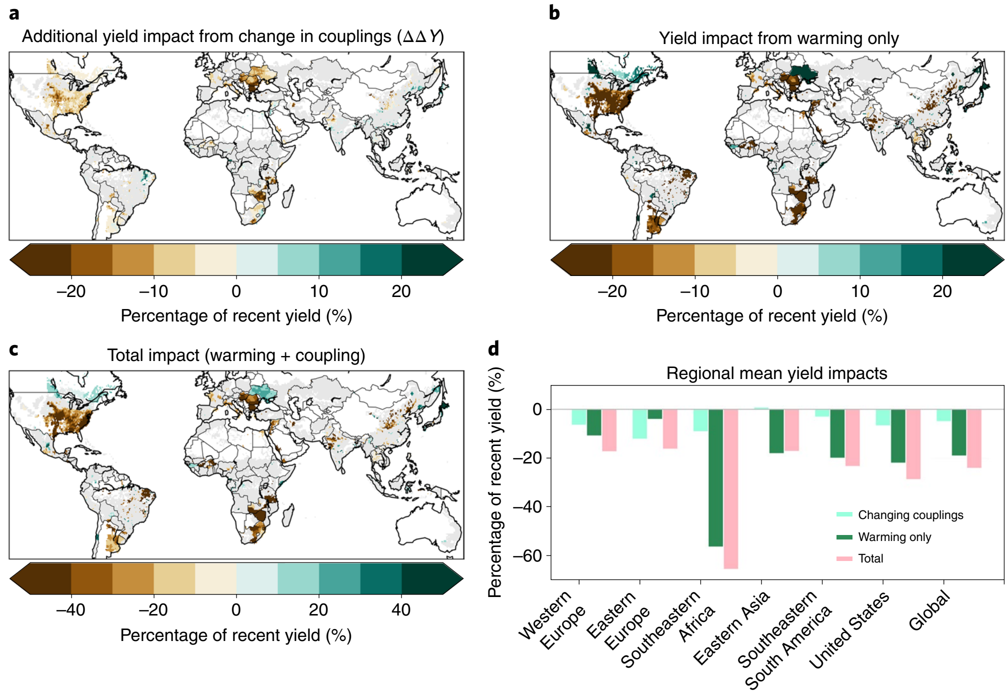

Fig. 5 | Projected additional impact of future warming on maize yields due to changing temperature–moisture couplings. a, Ensemble median additional impact of warming on maize yields from projected changes in $r_{T,ET}$ and $r_{T,p}$ over 2051–2100 under a moderate-emissions scenario (SSP2-4.5), as a percentage of the local mean of recent yields (2004–2013). **b**, Maize yield changes (as a percentage of recent yield) from ensemble median warming only, projected using historical yield sensitivity to temperature from Fig. 1a. **c**, Projected total yield impacts, estimated as the sum of impacts from changing couplings and warming only (note that the scale differs from that in **a** and **b**). The projections in **a**–**c** are shown only for areas with significant historical maize yield sensitivity to temperature ($P < 0.1$); the grey shading shows croplands with insignificant yield dependence on temperature. **d**, Yield impacts averaged across selected key regions and globally. The model uncertainties associated with these ensemble median results are shown in Fig. 6.

of 1% (3%) in eastern Asia (Fig. 5a,d and Supplementary Fig. 2). We note important model uncertainty in these regional figures, which we discuss further below and in Fig. 6d. More severe localized yield impacts at subregional scales reach ~20% in the United States and ~40% in eastern Europe and southeastern Africa.

These projected additional yield impacts due to changing temperature–moisture couplings ($\Delta\Delta Y$) would add to projected yield losses from warming alone (Fig. 5b), worsening them in some regions (for example, in the central United States) but slightly ameliorating them in others (for example, in eastern Asia, Fig. 5c). In some cool climates such as in the northern United States, Canada and Ukraine, changing couplings may also curtail projected yield gains from warming. Globally, we project that changing couplings will aggravate the impact of warming on maize and soy yields by ~5% relative to recent yields (Fig. 5d and Supplementary Fig. 2), evincing an important but underappreciated risk to agriculture under climate change.

Considerable intermodel variation underlies these multimodel median projections[20]. Over much of global maize croplands, fewer than two-thirds of models agree on the sign of additional yield changes due to coupling responses to warming ($\Delta\Delta Y$, Fig. 6a), especially in the tropics and subtropics. Even in areas with high model agreement on sign (mainly in Europe, the United States and eastern Asia), the magnitude of change can vary substantially across models (Fig. 6d and Supplementary Fig. 3). This intermodel variability introduces uncertainty in the projected global mean impacts for the moderate-emissions scenario, with model-specific yield impacts ranging from −17 to 11% (Fig. 6b, blue bars).

Alternate emissions scenarios add a further dimension of uncertainty to the projected yield impacts of changing temperature–moisture couplings. Under a high-emissions scenario (SSP5-8.5), maize yield losses in the Americas and southeastern Africa are reduced and gains in Asia are increased compared with the moderate-emissions scenario (Fig. 6c,d). Surprisingly, these regional responses amount to a global mean additional yield gain ($\Delta\Delta Y$) of 1.6% in the ensemble median ('additional' in that they only slightly offset large yield loss from warming itself). The counterintuitive non-monotonicity of the global mean response to emissions is ultimately driven by regional coupling changes that alleviate yield sensitivity to temperature, most notably the widespread relative decoupling between T and p under higher emissions (Supplementary Fig. 4). However, we also note large model disagreement in the high-emissions scenario, with global mean impacts ranging from −18 to 32% (Fig. 6b, red bars).

The uncertainties in these projections highlight unresolved challenges in simulating temperature–moisture couplings using climate models and their importance to predicting the impact of climate change on global crop production. Specifically, the responses of ET (largely mediated by soil and vegetation dynamics and land–atmosphere interaction) and precipitation (largely mediated by regional circulation) to interannual variability in temperature in future climates are both active areas of research[33,40–42]. While some regions with model consensus may reflect predictions with strong physical foundations, such as the enhanced land–atmosphere coupling in Europe with warming[22,43], they may also arise from stronger observational constraints and model validation effort across the northern midlatitudes[20,44]. Some regions lacking model consensus include important breadbaskets in southeast South America and chronically food-insecure and drought-vulnerable southeastern Africa, where weather observations are comparatively sparse and couplings are not well constrained by observations[20] (Fig. 6 and

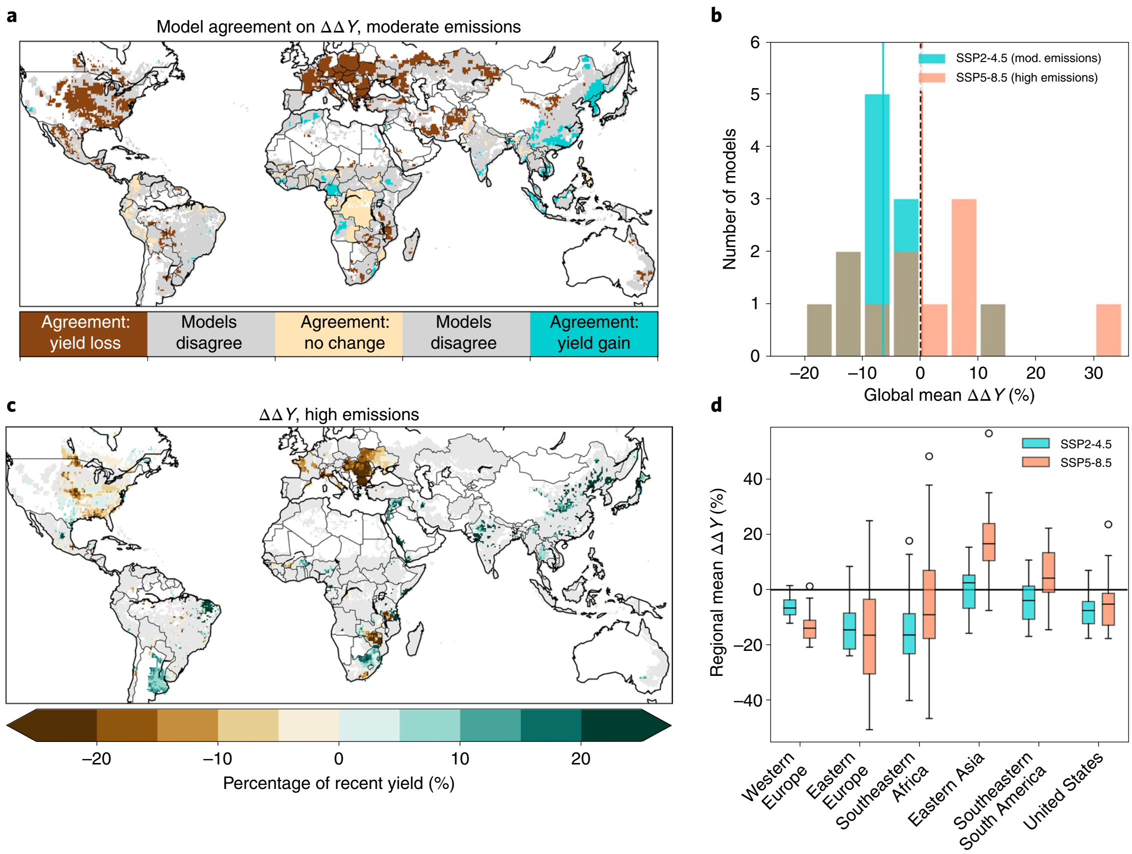

Fig. 6 | Uncertainty in projected additional maize yield impact due to changing temperature–moisture couplings. a, Model agreement on the local sign of projected additional yield impact due to changing temperature–moisture couplings (ΔΔ*Y*) under a moderate-emissions scenario by 2051–2100. The colouring denotes areas where at least two-thirds (8 of 12) of the models in the ensemble agree on positive (blue), negative (brown) or no substantial change (within +/−10%, beige). Grey denotes areas with less than two-thirds model agreement on the direction of change. **b**, Distribution of model-specific global mean ΔΔ*Y* for the moderate emissions (SSP2-4.5, blue) and high emissions (SSP5-8.5, red) scenarios. The vertical red and blue lines denote multimodel median global mean impacts. Additional yield impacts are expressed as percentages of 2004–2013 mean yields, averaged over areas with significant temperature effects on yield (Fig. 1a). Overlap between moderate- and high-emissions scenario outcome distributions (that is, where blue and red bars overlap) are shown as brown shading. **c**, Ensemble median additional impact of warming on maize yields due to changes in couplings over 2051–2100 under the high-emissions scenario (SSP5-8.5), as a percentage of the local mean of recent yields (2004–2013). The projections are shown only for areas with significant historical maize yield sensitivity to temperature ($P < 0.1$); the grey shading shows croplands with insignificant yield dependence on temperature. **d**, Distributions of model-specific regional mean ΔΔ*Y* for the moderate emissions (SSP2-4.5, blue) and high emissions (SSP5-8.5, red) scenarios. In each box plot, the centre line denotes the multimodel median, the whiskers indicate tail projections within 1.5× the interquartile range and the points indicate outlier projections.

Supplementary Fig. 3). These regions also tend to have the largest differences in estimated historic couplings between CMIP6 and observation-based data (Supplementary Fig. 5). Our results show how these uncertainties and potential model inaccuracies presently impede a complete understanding of the risks of climate change to crop production.

Several limitations of our study reflect important challenges and open questions. First, while we assess seasonal-scale yield responses and temperature–moisture couplings, future studies may consider subseasonal timescales, particularly the role of the couplings in short-duration heat extremes and flash droughts[43,45], and the differential vulnerability of crop growth stages. Second, we treat crops as passively affected by these couplings, but in some densely cropped regions, they actively influence climate by modifying regional ET[46,47]. While this occurrence is limited to certain high-yielding regions at present, it may become increasingly common with continued crop intensification and thus merits further attention. Third, while we treat circulation and land–atmosphere couplings as distinct, the influence of their overlap and interaction on past and future crop yield sensitivity to temperature should be investigated[18,41]. Fourth, future work should consider the uncertain impact of increased atmospheric CO_2 on future crop responses to combined heat and moisture stresses[48,49], which may weaken or amplify the relationships in Fig. 2 by increasing the water use efficiency of crops (yield per unit water transpired). Finally, further attention to the role of natural vegetation, aerosols and climate modes such as the El Niño/Southern Oscillation in temperature–moisture couplings is also merited[33,34].

Conclusion

Limitations and uncertainties in the climate models notwithstanding, we draw the following main conclusions from our results. Local heat sensitivity of crop yields depends on the strength of coupling between temperature and moisture for maize and soy, but not for rice and wheat. We propose that this dependence, and its absence for rice and wheat, is consistent with the compounding of heat impacts by moisture stress where couplings are strong, and mitigation where they are weak. By 2051–2100, enhanced couplings over a majority of global cropland will most likely make crops more vulnerable to warming temperatures, with notable exceptions across Asia, where couplings weaken. These climate impacts on crops are widely omitted from climate risk assessments.

Our projections of a mounting threat to crop yields from changing temperature–moisture couplings in a warming climate underscore the need to adapt global crop management and genetics to concurrent heat and moisture stresses. Cropping adaptations (such as breeding for drought and heat tolerance) should thus avoid antagonisms between stress mechanisms where couplings strengthen in the future[8,50], but may leverage them where couplings weaken. For instance, irrigation may disrupt the antagonistic feedbacks that lead to compounding heat and moisture stresses, so its effectiveness as a crop adaptation to heat may be enhanced where couplings get stronger in the future. However, the reliability of irrigation may simultaneously decline with strengthening couplings, as drought increasingly limits the availability of water for irrigation during extreme heat (that is, when it is needed most). As another example, breeding crops for drought tolerance based on stomatal regulation[35,37] or sowing density[51] may exacerbate heat impacts by reducing canopy evaporative cooling or raising crop water demand, respectively, a risk that would be less important where couplings weaken (as in much of Asia). Finally, our results may help further calibrate joint temperature–moisture impacts in crop models to assure their usefulness in developing climate-adaptive cropping strategies[14,52].

Efforts to adapt cropping to climates with increasingly strong temperature–moisture couplings may prioritize subsistence cropping areas that are already prone to drought and heat, and where we project that enhanced couplings will worsen crop vulnerability in the future. Even with robust adaptations, changes in crop sensitivity to heat under climate change will probably necessitate greater international cooperation in equitable food trade and emergency relief as climate shocks increase.

Methods

Data and processing. For the historical climate analyses, we combine monthly 0.5° gridded mean temperature and total precipitation observations from the Hadley Center Climate Research Unit (CRU TS4.02)[53] with 0.25° modelled mean temperature and ET data from Global Land Data Assimilation System (GLDAS) Noah land surface model L4, version 2.0 (ref. [54]). We coarsen the ET data from 0.25° to 0.5° to match the resolution of the temperature and precipitation data. To represent growing season mean conditions, we average temperature and ET and sum precipitation during the average crop-specific growing periods based on a global crop calendar[55]. For wheat, we define the growing season as three months before harvest to exclude the vernalization period for winter wheat. Because ET is the input data with the greatest observational limitations, we verified the robustness of key parameters estimated via the regression model in equation (2) to three alternative historical ET datasets: (1) GLDAS v.2.0 Catchment Land System Model L4 over 1961–2010 (ref. [54]), (2) GLDAS v.2.0 Variable Infiltration Capacity L4 over 1961–2010 (ref. [54]) and (3) ERA5 Reanalysis over 1980–2010 (ref. [56]).

The crop yield data are based on statistics from ~20,000 subnational political units over 1970–2013, harmonized for consistency with United Nations Food and Agriculture Organization national statistics and gridded to 0.5° resolution[26]. Harmonizing the subnational statistics with national Food and Agriculture Organization data ensures comparability between nations, but it may introduce discontinuities in the data along certain national boundaries, notably Ukraine. We focus on maize, wheat, rice and soy as crops that are globally dominant in calorie consumption and distributed across the world. For both the climate and crop data, we isolate interannual variability from longer-term trends using singular spectrum analysis, a non-parametric method that avoids assumptions about the functional form of the climate and yield trends[5,57].

Historical temperature–moisture couplings. To characterize the couplings between temperature and moisture, we compute grid-cell interannual Pearson's correlation coefficients between the detrended temperature and ET from GLDAS for the land–atmosphere coupling ($r_{T,\mathrm{ET}}$), and between temperature and precipitation from the Hadley Center Climate Research Unit for the circulation coupling ($r_{T,p}$). This approach leverages the strengths of observation-based data for $r_{T,p}$ but employs model-based data for ET, which is comparatively sparsely observed over global croplands[20,44]. To improve the robustness of interannual correlations with respect to important modes of climate variability such as the El Nino/Southern Oscillation, we use a somewhat longer 50-year period of 1961–2010 than the study period constrained by the yield data. We define the statistical significance of the couplings for each grid cell using a two-tailed t-test with a threshold of $P<0.1$.

For clarity, our nomenclature contrasts these two couplings on the basis of the dominant locus of their occurrence either in atmosphere dynamics or land–atmosphere interactions[18,19,21]. However, the two couplings interact physically in some regions and should not be considered strictly distinct[18,21,22]. For instance, global correlations between grid-cell $r_{T,\mathrm{ET}}$ and $r_{T,p}$ ($r^2=0.21$ for maize and 0.29 for soybean) may reflect links among p, ET and T in the coupled surface–atmosphere system that are not easily disentangled. Despite this, the magnitude of these correlations and the broadly divergent spatial pattern in their historic and projected future magnitude both suggest a prevailing differentiation of the two couplings. For brevity, we present the couplings only for maize in Fig. 1 and for the other crops in Supplementary Fig. 1, because their spatial patterns do not differ substantially across the different crops.

Historical crop yield sensitivity to heat. We estimate the historical yield sensitivity to temperature as the slope coefficient (β_T) in a simple linear regression model relating detrended yields to temperature for each grid cell:

$$y=\beta_0+\beta_T T+\varepsilon \tag{1}$$

where y denotes estimated yields, β_0 the intercept, T the mean seasonal temperature and ε the residual errors. Repeating this analysis for the four crops generates four maps of yield sensitivity to temperature. We standardize yield and temperature data such that β_T has units of standard deviations of yield per standard deviation of temperature (that is, it is dimensionless). This standardization eases the comparison of yield sensitivity across crop regions with different means and variances of yield and temperature.

The simplicity of this linear model of temperature impacts on yields eases the interpretation of the spatial patterns of impacts and the results of subsequent analyses, at the cost of reduced specificity between the impacts of beneficial and detrimental subseasonal temperatures that comprise the seasonal mean temperature. Despite this limitation, the spatial pattern and magnitude of estimated yield sensitivity largely agree with past studies using more complex models. For instance, we compare our unstandardized yield sensitivities aggregated to the national scale with those in the multimodel comparison of Zhao et al.[3] in Supplementary Fig. 8, and we find broadly consistent signs and magnitudes for top-producing countries for the four crops.

We define the statistical significance of the yield sensitivities for each grid cell using a two-tailed t-test with a threshold of $P<0.1$. Importantly, we do not interpret this yield sensitivity to reflect the response to heat stress alone; rather, it also reflects the response of crops to temperature via its impact on vapour pressure deficit, a key variable in moisture stress[2,7,13]. We conduct this analysis for all grid cells with non-zero crop area to leverage the largest possible diversity of climates and crop systems, regardless of their areal intensiveness.

Historical impact of temperature–moisture couplings on yield. Next, we assess the dependence of standardized yield sensitivity to temperature on the two historical coupling measures using a multiple linear regression model of the form

$$\beta_T=\alpha_0+\alpha_{T,\mathrm{ET}}r_{T,\mathrm{ET}}+\alpha_{T,p}r_{T,p}+\varepsilon \tag{2}$$

where $\alpha_{T,\mathrm{ET}}$ and $\alpha_{T,p}$ reflect the response of yield sensitivity to each coupling ($r_{T,\mathrm{ET}}$ and $r_{T,p}$), α_0 is the intercept, and ε is the residual errors. This method aggregates local yield sensitivities and coupling strengths into a dataset for each crop, and the regression results in two global estimates of the yield sensitivity response to each coupling ($\alpha_{T,\mathrm{ET}}$ and $\alpha_{T,p}$) for each crop. Because they represent change in a standardized coefficient per unit change in correlation, $\alpha_{T,\mathrm{ET}}$ and $\alpha_{T,p}$ are dimensionless. We include all grid cells with non-zero crop area and significant yield sensitivities to temperature ($P<0.1$) in this analysis, and we note that the regression results are highly robust to a stricter significance threshold of $P<0.05$ (Supplementary Fig. 9). On the basis of a minimum threshold for the coefficient of determination (r^2) of 0.2, we judge whether the couplings are substantially predictive of yield sensitivities for each crop, and we proceed with future projections only for crops that meet this criterion. Variance inflation factors for the models in equation (2) were 1.2–1.3, indicating low susceptibility of the coefficient estimates to the moderate collinearity between $r_{T,\mathrm{ET}}$ and $r_{T,p}$ ($r^2\approx0.2$–0.3). The estimated model parameters were broadly robust to alternative historical ET datasets, including Variable Infiltration Capacity and Catchment Land System Model land models from GLDAS and the ERA5 reanalysis (Supplementary Fig. 6).

Projecting future changes in couplings. To assess future changes in the couplings, we employ projected monthly mean temperature and ET and monthly total precipitation from a suite of CMIP6 general circulation models, run under the SSP2-4.5 moderate-emissions scenario[39]. We use all 12 models for which ET data are complete and available. The projected climate data are aggregated to the local growing season. We detrend the seasonal time series using singular spectrum analysis to remove the large influence of long-term forced trends in the climate variables, and we regrid the data to a common 0.5° resolution. Despite the lower native resolution of many climate models, we proceed with this higher resolution to conserve the spatial detail of historical mean yields and yield sensitivities to temperature, which are based on higher-resolution data. However, we avoid introducing non-physical results to our downscaled climate projections by using nearest-neighbour approximation rather than interpolating. This method essentially conserves the original model resolution in the climate component of our projections without sacrificing the higher resolution of the observed variables.

To project future changes in the temperature–moisture couplings, we compute $r_{T,\mathrm{ET}}$ and $r_{T,p}$ in the climate model data for both the historical period 1961–2010 and a future period of 2051–2100. We select the latter period to be distant enough in the future for climate signals to clearly emerge, but close enough to be useful for adaptation planning. We then compute a multimodel ensemble of correlation change factors by differencing the correlations between the historical and future periods. This differencing approach eliminates extraneous influence of historical mean model biases compared with observations (Supplementary Fig. 5), isolating the relative change in couplings projected by each model relative to its own historical period. Despite this, we note that historical biases probably reflect incomplete model simulation of the processes relevant to changes in the couplings. To represent the central tendency of the projection ensemble, we use the multimodel medians of projected change factors in the couplings ($\Delta r_{T,\mathrm{ET}}$ and $\Delta r_{T,p}$).

Projecting the crop yield impacts of changing couplings. We use the historical estimated coefficients relating yield sensitivity to temperature with each coupling ($\alpha_{T,\mathrm{ET}}$ and $\alpha_{T,p}$ in equation (2)) to project future changes in yield sensitivity to temperature ($\Delta\beta_T$) resulting from changes in the couplings, following

$$\Delta\beta_T = \alpha_{T,\mathrm{ET}}\Delta r_{T,\mathrm{ET}} + \alpha_{T,p}\Delta r_{T,p} \quad (3)$$

This equation employs the regression relation estimated in equation (2) but allows the coupling strength at each grid cell to change on the basis of the climate model projections. The central assumption in this approach is that the future yield sensitivity of each grid cell responds to future changes in the couplings at the global rates dictated by $\alpha_{T,\mathrm{ET}}$ and $\alpha_{T,p}$. We note that successful crop adaptation may challenge this assumption (Conclusion).

To ease the physical interpretation of the projected yield impacts, we convert the projected change in yield sensitivity to dimensional terms using

$$\Delta B_T = \Delta\beta_T \frac{\sigma_Y}{\sigma_T} \quad (4)$$

where ΔB_T coefficients have units of tons per ha per °C. We then project additional yield impacts of warming for each grid cell due to changes in coupling ($\Delta\Delta Y$) by multiplying this coefficient by the multimodel median of the mean seasonal warming by 2051–2100 (ΔT, computed by differencing modelled mean seasonal temperatures between the future and historical periods):

$$\Delta\Delta Y = \Delta B_T \Delta T \quad (5)$$

We present this additional yield impact as a percentage of recent local yields averaged over 2004–2013, the ten most recent years in our dataset, to contextualize the changes relative to local baseline yields. Finally, we average the percent yield changes across all grid cells with significant historical yield sensitivities to estimate net global additional yield impacts due to future changes in temperature–moisture couplings. Note that we map $\Delta r_{T,\mathrm{ET}}$, and $\Delta r_{T,p}$ over the full global cropland, regardless of the significance of historical yield sensitivities, to enable the interpretation of wider global patterns of change. However, we map $\Delta\Delta Y$ and $\Delta\beta_T$ only where historical yield sensitivity to temperature (β_T) is significant ($P<0.1$). We also show projected yield change from warming alone to contextualize $\Delta\Delta Y$; however, we do not consider these projections themselves to be a methodological improvement on past statistical yield projections using more complex models.

To assess uncertainty across the ensemble of climate models, we recompute equations (3)–(5) using model-specific changes in the couplings, rather than the ensemble median. We use a consistent multimodel median warming to compute additional yield impact so that the uncertainty analysis isolates differences between model-specific projected changes in couplings, rather than model differences in mean warming. This approach assumes that, at the seasonal scale, the influence of coupling changes on mean warming in each model is small relative to the radiative effect of greenhouse gases and dominant climate feedbacks (for example, ocean and cloud responses to warming)[43].

We then assess model agreement on the sign of the yield change for each grid cell. To do so, we classify whether at least eight models (two-thirds of the ensemble) project positive change (>10% yield gain), negative change (>10% yield loss) or little change (<10% yield gain or loss). Grid cells where fewer than eight models agree on the direction of change are classified as areas with substantial model disagreement. We also present histograms of model-specific projected net mean global yield change to reflect the distribution of plausible future global impacts. To account for uncertainty over future emissions, we include in this histogram equivalent results for a high-emissions scenario, SSP5-8.5 (ref. [39]). We also present $\Delta\Delta Y$ for this scenario to understand the spatial pattern of changes.

Finally, we present $\Delta\Delta Y$ for the two emissions scenarios averaged over several regions with noteworthy vulnerability or global importance. The data and methods used in this study are summarized visually in Supplementary Fig. 7. The base maps in Figs. 1 and 4–6 were developed by Generic Mapping Tools and used under a creative commons license.

Reporting Summary. Further information on research design is available in the Nature Research Reporting Summary linked to this article.

Data availability

The datasets supporting the results of this paper are freely available from the references and links listed in Supplementary Table 1. The crop yield data are available from D.R. upon request. The intermediate datasets are available at https://github.com/clesk/couplings-heat-crops. Source data are provided with this paper.

Code availability

The processing and analysis codes are available at https://github.com/clesk/couplings-heat-crops.

Received: 18 November 2020; Accepted: 8 July 2021;
Published online: 20 September 2021

References

1. Lobell, D. B. & Field, C. B. Global scale climate-crop yield relationships and the impacts of recent warming. *Environ. Res. Lett.* **2**, 014002 (2007).
2. Lobell, D. B. et al. The critical role of extreme heat for maize production in the United States. *Nat. Clim. Change* **3**, 497–501 (2013).
3. Zhao, C. et al. Temperature increase reduces global yields of major crops in four independent estimates. *Proc. Natl Acad. Sci. USA* **114**, 9326–9331 (2017).
4. Schlenker, W. & Roberts, M. J. Nonlinear temperature effects indicate severe damages to U.S. crop yields under climate change. *Proc. Natl Acad. Sci. USA* **106**, 15594–15598 (2009).
5. Vogel, E. et al. The effects of climate extremes on global agricultural yields. *Environ. Res. Lett.* **14**, 054010 (2019).
6. Lobell, D. B., Bänziger, M., Magorokosho, C. & Vivek, B. Nonlinear heat effects on African maize as evidenced by historical yield trials. *Nat. Clim. Change* **1**, 42–45 (2011).
7. Urban, D. W., Sheffield, J. & Lobell, D. B. The impacts of future climate and carbon dioxide changes on the average and variability of US maize yields under two emission scenarios. *Environ. Res. Lett.* **10**, 045003 (2015).
8. Prasad, P. V. V. et al. in *Response of Crops to Limited Water: Understanding and Modeling Water Stress Effects on Plant Growth Processes* (eds Ahuja, L. R. et al.) 301–356 (American Society of Agronomy, Crop Science Society of America, Soil Science Society of America, 2008); https://doi.org/10.2134/advagricsystmodel1.c11
9. Troy, T. J., Kipgen, C. & Pal, I. The impact of climate extremes and irrigation on US crop yields. *Environ. Res. Lett.* **10**, 054013 (2015).
10. Carter, E. K., Melkonian, J., Riha, S. J. & Shaw, S. B. Separating heat stress from moisture stress: analyzing yield response to high temperature in irrigated maize. *Environ. Res. Lett.* **11**, 094012 (2016).
11. Matiu, M., Ankerst, D. P. & Menzel, A. Interactions between temperature and drought in global and regional crop yield variability during 1961-2014. *PLoS ONE* **12**, e0178339 (2017).
12. Coffel, E. D. et al. Future hot and dry years worsen Nile Basin water scarcity despite projected precipitation increases. *Earth's Future* **7**, 967–977 (2019).
13. Rigden, A. J., Mueller, N. D., Holbrook, N. M., Pillai, N. & Huybers, P. Combined influence of soil moisture and atmospheric evaporative demand is important for accurately predicting US maize yields. *Nat. Food* **1**, 127–133 (2020).
14. Schauberger, B. et al. Consistent negative response of US crops to high temperatures in observations and crop models. *Nat. Commun.* **8**, 13931 (2017).
15. Ortiz-Bobea, A., Wang, H., Carrillo, C. M. & Ault, T. R. Unpacking the climatic drivers of US agricultural yields. *Environ. Res. Lett.* **14**, 064003 (2019).
16. Siebert, S., Webber, H., Zhao, G. & Ewert, F. Heat stress is overestimated in climate impact studies for irrigated agriculture. *Environ. Res. Lett.* **12**, 044012 (2017).
17. Lesk, C. & Anderson, W. Decadal variability modulates trends in concurrent heat and drought over global croplands. *Environ. Res. Lett.* 16 055024 (2021).
18. Berg, A. et al. Interannual coupling between summertime surface temperature and precipitation over land: processes and implications for climate change. *J. Clim.* **28**, 1308–1328 (2015).
19. Seneviratne, S. I. et al. Investigating soil moisture–climate interactions in a changing climate: a review. *Earth Sci. Rev.* **99**, 125–161 (2010).
20. Zscheischler, J. & Seneviratne, S. I. Dependence of drivers affects risks associated with compound events. *Sci. Adv.* **3**, e1700263 (2017).
21. Trenberth, K. E. & Shea, D. J. Relationships between precipitation and surface temperature. *Geophys. Res. Lett.* **32**, 1–4 (2005).

22. Seneviratne, S. I., Lüthi, D., Litschi, M. & Schär, C. Land–atmosphere coupling and climate change in Europe. *Nature* **443**, 205–209 (2006).
23. Horton, R. M., Mankin, J. S., Lesk, C., Coffel, E. & Raymond, C. A review of recent advances in research on extreme heat events. *Curr. Clim. Change Rep.* **2**, 242–259 (2016).
24. Berg, A. et al. Impact of soil moisture–atmosphere interactions on surface temperature distribution. *J. Clim.* **27**, 7976–7993 (2014).
25. Miralles, D. G., Teuling, A. J., Van Heerwaarden, C. C. & De Arellano, J. V. G. Mega-heatwave temperatures due to combined soil desiccation and atmospheric heat accumulation. *Nat. Geosci.* **7**, 345–349 (2014).
26. Ray, D. K. et al. Climate change has likely already affected global food production. *PLoS ONE* **14**, e0217148 (2019).
27. Ray, D. K., Gerber, J. S., Macdonald, G. K. & West, P. C. Climate variation explains a third of global crop yield variability. *Nat. Commun.* **6**, 5989 (2015).
28. Liu, B. et al. Similar estimates of temperature impacts on global wheat yield by three independent methods. *Nat. Clim. Change* **6**, 1130–1136 (2016).
29. Sánchez, B., Rasmussen, A. & Porter, J. R. Temperatures and the growth and development of maize and rice: a review. *Glob. Change Biol.* **20**, 408–417 (2014).
30. Welch, J. R. et al. Rice yields in tropical/subtropical Asia exhibit large but opposing sensitivities to minimum and maximum temperatures. *Proc. Natl Acad. Sci. USA* **107**, 14562–14567 (2010).
31. Zhang, T., Lin, X. & Sassenrath, G. F. Current irrigation practices in the central United States reduce drought and extreme heat impacts for maize and soybean, but not for wheat. *Sci. Total Environ.* **508**, 331–342 (2015).
32. Mittler, R. Abiotic stress, the field environment and stress combination. *Trends Plant Sci.* **11**, 15–19 (2006).
33. Swann, A. L. S. Plants and drought in a changing climate. *Curr. Clim. Change Rep.* **4**, 192–201 (2018).
34. Skinner, C. B., Poulsen, C. J. & Mankin, J. S. Amplification of heat extremes by plant CO_2 physiological forcing. *Nat. Commun.* **9**, 1–11 (2018).
35. Gates, D. M. Transpiration and leaf temperature. *Annu. Rev. Plant Physiol.* **19**, 211–238 (1968).
36. Crafts-Brandner, S. J. & Salvucci, M. E. Sensitivity of photosynthesis in a C_4 plant, maize, to heat stress. *Plant Physiol.* **129**, 1773–1780 (2002).
37. Grossiord, C. et al. Plant responses to rising vapor pressure deficit. *N. Phytol.* **226**, 1550–1566 (2020).
38. Rosenzweig, C. et al. Assessing agricultural risks of climate change in the 21st century in a global gridded crop model intercomparison. *Proc. Natl Acad. Sci. USA* **111**, 3268–3273 (2014).
39. Eyring, V. et al. Overview of the Coupled Model Intercomparison Project Phase 6 (CMIP6) experimental design and organization. *Geosci. Model Dev.* **9**, 1937–1958 (2016).
40. Seth, A. et al. Monsoon responses to climate changes—connecting past, present and future. *Curr. Clim. Change Rep.* 5, 63–79 (2019).
41. Orlowsky, B. & Seneviratne, S. I. Statistical analyses of land–atmosphere feedbacks and their possible pitfalls. *J. Clim.* **23**, 3918–3932 (2010).
42. Lesk, C., Coffel, E. & Horton, R. Net benefits to US soy and maize yields from intensifying hourly rainfall. *Nat. Clim. Change* **10**, 819–822 (2020).
43. Vogel, M. M. et al. Regional amplification of projected changes in extreme temperatures strongly controlled by soil moisture–temperature feedbacks. *Geophys. Res. Lett.* **44**, 1511–1519 (2017).
44. Mueller, B. et al. Evaluation of global observations-based evapotranspiration datasets and IPCC AR4 simulations. *Geophys. Res. Lett.* **38**, 1–7 (2011).
45. Pendergrass, A. G. et al. Flash droughts present a new challenge for subseasonal-to-seasonal prediction. *Nat. Clim. Change* **10**, 191–199 (2020).
46. Mueller, N. D. et al. Global relationships between cropland intensification and summer temperature extremes over the last 50 years. *J. Clim.* **30**, 7505–7528 (2017).
47. He, Y., Lee, E. & Mankin, J. S. Seasonal tropospheric cooling in northeast China associated with cropland expansion. *Environ. Res. Lett.* **15**, 034032 (2020).
48. Ainsworth, E. A. & Long, S. P. 30 years of free-air carbon dioxide enrichment (FACE): what have we learned about future crop productivity and its potential for adaptation? *Glob. Change Biol.* **27**, 27–49 (2021).
49. Deryng, D. et al. Regional disparities in the beneficial effects of rising CO_2 concentrations on crop water productivity. *Nat. Clim. Change* **6**, 786–790 (2016).
50. Challinor, A. J., Koehler, A.-K., Ramirez-Villegas, J., Whitfield, S. & Das, B. Current warming will reduce yields unless maize breeding and seed systems adapt immediately. *Nat. Clim. Change* **6**, 954–958 (2016).
51. Lobell, D. B., Deines, J. M. & Di Tommaso, S. Changes in the drought sensitivity of US maize yields. *Nat. Food* **1**, 729–735 (2020).
52. Bassu, S. et al. How do various maize crop models vary in their responses to climate change factors? *Glob. Change Biol.* **20**, 2301–2320 (2014).
53. Harris, I., Jones, P. D., Osborn, T. J. & Lister, D. H. Updated high-resolution grids of monthly climatic observations—the CRU TS3.10 dataset. *Int. J. Clim.* **34**, 623–642 (2014).
54. Rodell, M. et al. The Global Land Data Assimilation System. *Bull. Am. Meteorol. Soc.* **85**, 381–394 (2004).
55. Sacks, W. J., Deryng, D. & Foley, J. A. Crop planting dates: an analysis of global patterns. *Glob. Ecol. Biogeogr.* **19**, 607–620 (2010).
56. Hersbach, H. et al. The ERA5 global reanalysis. *Q. J. R. Meteorol. Soc.* **146**, 1999–2049 (2020).
57. Vautard, R., Yiou, P. & Ghil, M. Singular-spectrum analysis: a toolkit for short, noisy chaotic signals. *Physica D* **58**, 95–126 (1992).

Acknowledgements

This material is based on work supported by the National Science Foundation Graduate Research Fellowship under grant no. DGE—1644869. J.W. was supported by the National Science Foundation under grant no. BCS—184018. J.Z. acknowledges the Swiss National Science Foundation (Ambizione grant no. 179876) and the Helmholtz Initiative and Networking Fund (Young Investigator Group COMPOUNDX, grant agreement no. VH-NG-1537). S.I.S. acknowledges support from the European Union's Horizon 2020 Research and Innovation Program (grant agreement no. 821003 (4C)) and the Swiss National Foundation in relation to the DAMOCLES COST Action (project 'Compound events in a changing climate'). We thank J. Jägermeyr, J. Mankin, R. DeFries and M. Ting for constructive feedback on the methods and results. We acknowledge the World Climate Research Programme, which, through its Working Group on Coupled Modelling, coordinated CMIP6. We thank the climate modelling groups for producing and making available their model output, the Earth System Grid Federation (ESGF) for archiving the data, and the funding agencies who support CMIP6 and ESGF.

Author contributions

C.L., E.C. and J.W. designed and coordinated this research. C.L. conducted the analysis. All authors discussed the methods and results and wrote the manuscript.

Competing interests

The authors declare no competing interests.

Additional information

Supplementary information The online version contains supplementary material available at https://doi.org/10.1038/s43016-021-00341-6.

Correspondence and requests for materials should be addressed to Corey Lesk.

Peer review information *Nature Food* thanks Angeline Pendergrass and the other, anonymous, reviewer(s) for their contribution to the peer review of this work.

Reprints and permissions information is available at www.nature.com/reprints.

Publisher's note Springer Nature remains neutral with regard to jurisdictional claims in published maps and institutional affiliations.

nature research

Corresponding author(s): *Double-blind peer review submissions: write DBPR and your manuscript number here instead of author names.*

Last updated by author(s): *YYYY-MM-DD*

Reporting Summary

Nature Research wishes to improve the reproducibility of the work that we publish. This form provides structure for consistency and transparency in reporting. For further information on Nature Research policies, see our Editorial Policies and the Editorial Policy Checklist.

Statistics

For all statistical analyses, confirm that the following items are present in the figure legend, table legend, main text, or Methods section.

n/a	Confirmed	
☐	☐	The exact sample size (n) for each experimental group/condition, given as a discrete number and unit of measurement
☐	☐	A statement on whether measurements were taken from distinct samples or whether the same sample was measured repeatedly
☐	☐	The statistical test(s) used AND whether they are one- or two-sided *Only common tests should be described solely by name; describe more complex techniques in the Methods section.*
☐	☐	A description of all covariates tested
☐	☐	A description of any assumptions or corrections, such as tests of normality and adjustment for multiple comparisons
☐	☐	A full description of the statistical parameters including central tendency (e.g. means) or other basic estimates (e.g. regression coefficient) AND variation (e.g. standard deviation) or associated estimates of uncertainty (e.g. confidence intervals)
☐	☐	For null hypothesis testing, the test statistic (e.g. F, t, r) with confidence intervals, effect sizes, degrees of freedom and P value noted *Give P values as exact values whenever suitable.*
☐	☐	For Bayesian analysis, information on the choice of priors and Markov chain Monte Carlo settings
☐	☐	For hierarchical and complex designs, identification of the appropriate level for tests and full reporting of outcomes
☐	☐	Estimates of effect sizes (e.g. Cohen's d, Pearson's r), indicating how they were calculated

Our web collection on statistics for biologists contains articles on many of the points above.

Software and code

Policy information about availability of computer code

Data collection	*Provide a description of all commercial, open source and custom code used to collect the data in this study, specifying the version used OR state that no software was used.*
Data analysis	*Provide a description of all commercial, open source and custom code used to analyse the data in this study, specifying the version used OR state that no software was used.*

For manuscripts utilizing custom algorithms or software that are central to the research but not yet described in published literature, software must be made available to editors and reviewers. We strongly encourage code deposition in a community repository (e.g. GitHub). See the Nature Research guidelines for submitting code & software for further information.

Data

Policy information about availability of data

All manuscripts must include a data availability statement. This statement should provide the following information, where applicable:

- Accession codes, unique identifiers, or web links for publicly available datasets
- A list of figures that have associated raw data
- A description of any restrictions on data availability

Provide your data availability statement here.

Field-specific reporting

Please select the one below that is the best fit for your research. If you are not sure, read the appropriate sections before making your selection.

☐ Life sciences ☐ Behavioural & social sciences ☐ Ecological, evolutionary & environmental sciences

For a reference copy of the document with all sections, see nature.com/documents/nr-reporting-summary-flat.pdf

Life sciences study design

All studies must disclose on these points even when the disclosure is negative.

Sample size	*Describe how sample size was determined, detailing any statistical methods used to predetermine sample size OR if no sample-size calculation was performed, describe how sample sizes were chosen and provide a rationale for why these sample sizes are sufficient.*
Data exclusions	*Describe any data exclusions. If no data were excluded from the analyses, state so OR if data were excluded, describe the exclusions and the rationale behind them, indicating whether exclusion criteria were pre-established.*
Replication	*Describe the measures taken to verify the reproducibility of the experimental findings. If all attempts at replication were successful, confirm this OR if there are any findings that were not replicated or cannot be reproduced, note this and describe why.*
Randomization	*Describe how samples/organisms/participants were allocated into experimental groups. If allocation was not random, describe how covariates were controlled OR if this is not relevant to your study, explain why.*
Blinding	*Describe whether the investigators were blinded to group allocation during data collection and/or analysis. If blinding was not possible, describe why OR explain why blinding was not relevant to your study.*

Behavioural & social sciences study design

All studies must disclose on these points even when the disclosure is negative.

Study description	*Briefly describe the study type including whether data are quantitative, qualitative, or mixed-methods (e.g. qualitative cross-sectional, quantitative experimental, mixed-methods case study).*
Research sample	*State the research sample (e.g. Harvard university undergraduates, villagers in rural India) and provide relevant demographic information (e.g. age, sex) and indicate whether the sample is representative. Provide a rationale for the study sample chosen. For studies involving existing datasets, please describe the dataset and source.*
Sampling strategy	*Describe the sampling procedure (e.g. random, snowball, stratified, convenience). Describe the statistical methods that were used to predetermine sample size OR if no sample-size calculation was performed, describe how sample sizes were chosen and provide a rationale for why these sample sizes are sufficient. For qualitative data, please indicate whether data saturation was considered, and what criteria were used to decide that no further sampling was needed.*
Data collection	*Provide details about the data collection procedure, including the instruments or devices used to record the data (e.g. pen and paper, computer, eye tracker, video or audio equipment) whether anyone was present besides the participant(s) and the researcher, and whether the researcher was blind to experimental condition and/or the study hypothesis during data collection.*
Timing	*Indicate the start and stop dates of data collection. If there is a gap between collection periods, state the dates for each sample cohort.*
Data exclusions	*If no data were excluded from the analyses, state so OR if data were excluded, provide the exact number of exclusions and the rationale behind them, indicating whether exclusion criteria were pre-established.*
Non-participation	*State how many participants dropped out/declined participation and the reason(s) given OR provide response rate OR state that no participants dropped out/declined participation.*
Randomization	*If participants were not allocated into experimental groups, state so OR describe how participants were allocated to groups, and if allocation was not random, describe how covariates were controlled.*

Ecological, evolutionary & environmental sciences study design

All studies must disclose on these points even when the disclosure is negative.

Study description	*Briefly describe the study. For quantitative data include treatment factors and interactions, design structure (e.g. factorial, nested, hierarchical), nature and number of experimental units and replicates.*
Research sample	*Describe the research sample (e.g. a group of tagged Passer domesticus, all Stenocereus thurberi within Organ Pipe Cactus National*

Research sample	Monument), and provide a rationale for the sample choice. When relevant, describe the organism taxa, source, sex, age range and any manipulations. State what population the sample is meant to represent when applicable. For studies involving existing datasets, describe the data and its source.
Sampling strategy	Note the sampling procedure. Describe the statistical methods that were used to predetermine sample size OR if no sample-size calculation was performed, describe how sample sizes were chosen and provide a rationale for why these sample sizes are sufficient.
Data collection	Describe the data collection procedure, including who recorded the data and how.
Timing and spatial scale	Indicate the start and stop dates of data collection, noting the frequency and periodicity of sampling and providing a rationale for these choices. If there is a gap between collection periods, state the dates for each sample cohort. Specify the spatial scale from which the data are taken
Data exclusions	If no data were excluded from the analyses, state so OR if data were excluded, describe the exclusions and the rationale behind them, indicating whether exclusion criteria were pre-established.
Reproducibility	Describe the measures taken to verify the reproducibility of experimental findings. For each experiment, note whether any attempts to repeat the experiment failed OR state that all attempts to repeat the experiment were successful.
Randomization	Describe how samples/organisms/participants were allocated into groups. If allocation was not random, describe how covariates were controlled. If this is not relevant to your study, explain why.
Blinding	Describe the extent of blinding used during data acquisition and analysis. If blinding was not possible, describe why OR explain why blinding was not relevant to your study.

Did the study involve field work? ☐ Yes ☐ No

Field work, collection and transport

Field conditions	Describe the study conditions for field work, providing relevant parameters (e.g. temperature, rainfall).
Location	State the location of the sampling or experiment, providing relevant parameters (e.g. latitude and longitude, elevation, water depth).
Access & import/export	Describe the efforts you have made to access habitats and to collect and import/export your samples in a responsible manner and in compliance with local, national and international laws, noting any permits that were obtained (give the name of the issuing authority, the date of issue, and any identifying information).
Disturbance	Describe any disturbance caused by the study and how it was minimized.

Reporting for specific materials, systems and methods

We require information from authors about some types of materials, experimental systems and methods used in many studies. Here, indicate whether each material, system or method listed is relevant to your study. If you are not sure if a list item applies to your research, read the appropriate section before selecting a response.

Materials & experimental systems

n/a	Involved in the study
☐	☐ Antibodies
☐	☐ Eukaryotic cell lines
☐	☐ Palaeontology and archaeology
☐	☐ Animals and other organisms
☐	☐ Human research participants
☐	☐ Clinical data
☐	☐ Dual use research of concern

Methods

n/a	Involved in the study
☐	☐ ChIP-seq
☐	☐ Flow cytometry
☐	☐ MRI-based neuroimaging

Antibodies

Antibodies used	Describe all antibodies used in the study; as applicable, provide supplier name, catalog number, clone name, and lot number.
Validation	Describe the validation of each primary antibody for the species and application, noting any validation statements on the manufacturer's website, relevant citations, antibody profiles in online databases, or data provided in the manuscript.

Eukaryotic cell lines

Policy information about cell lines

Cell line source(s)	State the source of each cell line used.

Authentication	*Describe the authentication procedures for each cell line used OR declare that none of the cell lines used were authenticated.*
Mycoplasma contamination	*Confirm that all cell lines tested negative for mycoplasma contamination OR describe the results of the testing for mycoplasma contamination OR declare that the cell lines were not tested for mycoplasma contamination.*
Commonly misidentified lines (See ICLAC register)	*Name any commonly misidentified cell lines used in the study and provide a rationale for their use.*

Palaeontology and Archaeology

Specimen provenance	*Provide provenance information for specimens and describe permits that were obtained for the work (including the name of the issuing authority, the date of issue, and any identifying information).*
Specimen deposition	*Indicate where the specimens have been deposited to permit free access by other researchers.*
Dating methods	*If new dates are provided, describe how they were obtained (e.g. collection, storage, sample pretreatment and measurement), where they were obtained (i.e. lab name), the calibration program and the protocol for quality assurance OR state that no new dates are provided.*

☐ Tick this box to confirm that the raw and calibrated dates are available in the paper or in Supplementary Information.

Ethics oversight	*Identify the organization(s) that approved or provided guidance on the study protocol, OR state that no ethical approval or guidance was required and explain why not.*

Note that full information on the approval of the study protocol must also be provided in the manuscript.

Animals and other organisms

Policy information about studies involving animals; ARRIVE guidelines recommended for reporting animal research

Laboratory animals	*For laboratory animals, report species, strain, sex and age OR state that the study did not involve laboratory animals.*
Wild animals	*Provide details on animals observed in or captured in the field; report species, sex and age where possible. Describe how animals were caught and transported and what happened to captive animals after the study (if killed, explain why and describe method; if released, say where and when) OR state that the study did not involve wild animals.*
Field-collected samples	*For laboratory work with field-collected samples, describe all relevant parameters such as housing, maintenance, temperature, photoperiod and end-of-experiment protocol OR state that the study did not involve samples collected from the field.*
Ethics oversight	*Identify the organization(s) that approved or provided guidance on the study protocol, OR state that no ethical approval or guidance was required and explain why not.*

Note that full information on the approval of the study protocol must also be provided in the manuscript.

Human research participants

Policy information about studies involving human research participants

Population characteristics	*Describe the covariate-relevant population characteristics of the human research participants (e.g. age, gender, genotypic information, past and current diagnosis and treatment categories). If you filled out the behavioural & social sciences study design questions and have nothing to add here, write "See above."*
Recruitment	*Describe how participants were recruited. Outline any potential self-selection bias or other biases that may be present and how these are likely to impact results.*
Ethics oversight	*Identify the organization(s) that approved the study protocol.*

Note that full information on the approval of the study protocol must also be provided in the manuscript.

Clinical data

Policy information about clinical studies
All manuscripts should comply with the ICMJE guidelines for publication of clinical research and a completed CONSORT checklist must be included with all submissions.

Clinical trial registration	*Provide the trial registration number from ClinicalTrials.gov or an equivalent agency.*
Study protocol	*Note where the full trial protocol can be accessed OR if not available, explain why.*
Data collection	*Describe the settings and locales of data collection, noting the time periods of recruitment and data collection.*
Outcomes	*Describe how you pre-defined primary and secondary outcome measures and how you assessed these measures.*

Dual use research of concern

Policy information about dual use research of concern

Hazards

Could the accidental, deliberate or reckless misuse of agents or technologies generated in the work, or the application of information presented in the manuscript, pose a threat to:

No	Yes	
☐	☐	Public health
☐	☐	National security
☐	☐	Crops and/or livestock
☐	☐	Ecosystems
☐	☐	Any other significant area

Experiments of concern

Does the work involve any of these experiments of concern:

No	Yes	
☐	☐	Demonstrate how to render a vaccine ineffective
☐	☐	Confer resistance to therapeutically useful antibiotics or antiviral agents
☐	☐	Enhance the virulence of a pathogen or render a nonpathogen virulent
☐	☐	Increase transmissibility of a pathogen
☐	☐	Alter the host range of a pathogen
☐	☐	Enable evasion of diagnostic/detection modalities
☐	☐	Enable the weaponization of a biological agent or toxin
☐	☐	Any other potentially harmful combination of experiments and agents

ChIP-seq

Data deposition

☐ Confirm that both raw and final processed data have been deposited in a public database such as GEO.

☐ Confirm that you have deposited or provided access to graph files (e.g. BED files) for the called peaks.

Data access links *May remain private before publication.*	*For "Initial submission" or "Revised version" documents, provide reviewer access links. For your "Final submission" document, provide a link to the deposited data.*
Files in database submission	*Provide a list of all files available in the database submission.*
Genome browser session (e.g. UCSC)	*Provide a link to an anonymized genome browser session for "Initial submission" and "Revised version" documents only, to enable peer review. Write "no longer applicable" for "Final submission" documents.*

Methodology

Replicates	*Describe the experimental replicates, specifying number, type and replicate agreement.*
Sequencing depth	*Describe the sequencing depth for each experiment, providing the total number of reads, uniquely mapped reads, length of reads and whether they were paired- or single-end.*
Antibodies	*Describe the antibodies used for the ChIP-seq experiments; as applicable, provide supplier name, catalog number, clone name, and lot number.*
Peak calling parameters	*Specify the command line program and parameters used for read mapping and peak calling, including the ChIP, control and index files used.*
Data quality	*Describe the methods used to ensure data quality in full detail, including how many peaks are at FDR 5% and above 5-fold enrichment.*
Software	*Describe the software used to collect and analyze the ChIP-seq data. For custom code that has been deposited into a community repository, provide accession details.*

Flow Cytometry

Plots

Confirm that:

- [ ] The axis labels state the marker and fluorochrome used (e.g. CD4-FITC).
- [ ] The axis scales are clearly visible. Include numbers along axes only for bottom left plot of group (a 'group' is an analysis of identical markers).
- [ ] All plots are contour plots with outliers or pseudocolor plots.
- [ ] A numerical value for number of cells or percentage (with statistics) is provided.

Methodology

Sample preparation	*Describe the sample preparation, detailing the biological source of the cells and any tissue processing steps used.*
Instrument	*Identify the instrument used for data collection, specifying make and model number.*
Software	*Describe the software used to collect and analyze the flow cytometry data. For custom code that has been deposited into a community repository, provide accession details.*
Cell population abundance	*Describe the abundance of the relevant cell populations within post-sort fractions, providing details on the purity of the samples and how it was determined.*
Gating strategy	*Describe the gating strategy used for all relevant experiments, specifying the preliminary FSC/SSC gates of the starting cell population, indicating where boundaries between "positive" and "negative" staining cell populations are defined.*

- [ ] Tick this box to confirm that a figure exemplifying the gating strategy is provided in the Supplementary Information.

Magnetic resonance imaging

Experimental design

Design type	*Indicate task or resting state; event-related or block design.*
Design specifications	*Specify the number of blocks, trials or experimental units per session and/or subject, and specify the length of each trial or block (if trials are blocked) and interval between trials.*
Behavioral performance measures	*State number and/or type of variables recorded (e.g. correct button press, response time) and what statistics were used to establish that the subjects were performing the task as expected (e.g. mean, range, and/or standard deviation across subjects).*

Acquisition

Imaging type(s)	*Specify: functional, structural, diffusion, perfusion.*
Field strength	*Specify in Tesla*
Sequence & imaging parameters	*Specify the pulse sequence type (gradient echo, spin echo, etc.), imaging type (EPI, spiral, etc.), field of view, matrix size, slice thickness, orientation and TE/TR/flip angle.*
Area of acquisition	*State whether a whole brain scan was used OR define the area of acquisition, describing how the region was determined.*

Diffusion MRI ☐ Used ☐ Not used

Preprocessing

Preprocessing software	*Provide detail on software version and revision number and on specific parameters (model/functions, brain extraction, segmentation, smoothing kernel size, etc.).*
Normalization	*If data were normalized/standardized, describe the approach(es): specify linear or non-linear and define image types used for transformation OR indicate that data were not normalized and explain rationale for lack of normalization.*
Normalization template	*Describe the template used for normalization/transformation, specifying subject space or group standardized space (e.g. original Talairach, MNI305, ICBM152) OR indicate that the data were not normalized.*
Noise and artifact removal	*Describe your procedure(s) for artifact and structured noise removal, specifying motion parameters, tissue signals and physiological signals (heart rate, respiration).*

Volume censoring | *Define your software and/or method and criteria for volume censoring, and state the extent of such censoring.*

Statistical modeling & inference

Model type and settings | *Specify type (mass univariate, multivariate, RSA, predictive, etc.) and describe essential details of the model at the first and second levels (e.g. fixed, random or mixed effects; drift or auto-correlation).*

Effect(s) tested | *Define precise effect in terms of the task or stimulus conditions instead of psychological concepts and indicate whether ANOVA or factorial designs were used.*

Specify type of analysis: ☐ Whole brain ☐ ROI-based ☐ Both

Statistic type for inference (See Eklund et al. 2016) | *Specify voxel-wise or cluster-wise and report all relevant parameters for cluster-wise methods.*

Correction | *Describe the type of correction and how it is obtained for multiple comparisons (e.g. FWE, FDR, permutation or Monte Carlo).*

Models & analysis

n/a	Involved in the study
☐	☐ Functional and/or effective connectivity
☐	☐ Graph analysis
☐	☐ Multivariate modeling or predictive analysis

Functional and/or effective connectivity | *Report the measures of dependence used and the model details (e.g. Pearson correlation, partial correlation, mutual information).*

Graph analysis | *Report the dependent variable and connectivity measure, specifying weighted graph or binarized graph, subject- or group-level, and the global and/or node summaries used (e.g. clustering coefficient, efficiency, etc.).*

Multivariate modeling and predictive analysis | *Specify independent variables, features extraction and dimension reduction, model, training and evaluation metrics.*